

FBG Optimization Using Spline Encoded Evolutionary Strategy

Marco José de Sousa, João Crisóstomo Weyl A. Costa,
Roberto Medeiros de Souza, Ramon Villar Monte Palma Pantoja
Laboratório de Eletromagnetismo Aplicado
Universidade Federal do Pará – UFPA
e-mail: {marcojsousa,jweyl}@ufpa.br

Abstract—This paper presents a chromosome encoding technique to be applied with Evolution Strategies (ES) or other population based optimization algorithms. The proposed encoding scheme uses spline approximations to build softened and ample refractive index profiles from few encoded parameters. This approach results in a dimensionality reduction and the respect of important restrictions associated to the FBG manufacture. Simulations are shown where an ES using the spline encoding is able to converge faster and produce more interesting filters, when compared with conventional encoding schemes.

I. INTRODUCTION

Fibre Bragg Gratings (FBGs) are flexible components. By adjusting the parameters that describes their refractive index profile, it is possible to obtain filters showing reflectance spectrum adapted to almost any type of application. Unfortunately this procedure (FBG synthesis) is not a trivial problem and several techniques have been proposed with some degree of success.

For example, if only weak gratings are considered, the refractive index profile can be obtained from the Fourier Transform of the reflection coefficient. This was the approach used by Winick and Roman [1] with interesting but inaccurate results. In the other hand, other techniques like these based on Layer Peeling (LP) [2][3] are capable of very accurate solutions in terms of reflectance spectrum, but have as side effect the generation of large and complex refractive index profiles that are difficult to built using Ultra Violet (UV) mask manufacture techniques [4]. In order to attend all restrictions associated to the FBG manufacture, Askanes et al [5] proposed an hybrid method that combines classical optimization techniques and the LP algorithm.

Other design alternatives are Evolutionary Algorithms (EA), Genetic Algorithm (GA) [6] and Particle Swarm Optimization (PSO) [7] allow to achieve satisfactory results even under heavy restrictions due to the manufacture process. For example, in [8], a pioneer article about the use of GAs for FBG synthesis, feasible Wavelength Division Multiplexing (WDM) filters with negligible dispersion are obtained. In [9], the FBG synthesis is performed using the Covariance Matrix Adapted Evolution Strategy (CMAES) with relative great success. Similar results are achieved in [10] using PSO. In [11], a GA is applied in the synthesis of Triangular FBGs

(TFBGs). In [12], the TFBG synthesis is performed again, but using the CMAES.

Although literature shows that meta-heuristics can be used to synthesize FBGs, they suffer because of the high number of parameters needed to represent a FBG properly. Using the modelling based on uniform sections presented in [13], an apodized FBG one centimetre long can be represented by about one hundred uniform sections, each one modelled by four parameters. Even considering a single parameter by section, about one hundred in total must be used to represent the entire FBG. This high dimensionality can make the meta-heuristic optimization scheme not practical. Frequently in the literature a FBG is designed with a very reduced number of uniform sections. For example, in [10], only 20 sections are considered. The use of a reduced number of sections can generate mismatches large enough to work like mirrors inside the FBG, which can create several cavities along the grating. In this case the reflectance spectrum can result noisy and full of undesired lobes, affecting the meta-heuristic convergence.

Therefore, it is interesting to produce softened refractive index profiles and find a way to do that using as few parameters as possible. Fortunately, according to the information theory, softened signal formats shall carry naturally less information and, consequently, it is possible to use less parameters to encode them. This article explores the use of spline approximations to create softened profiles from few points stored in ES individuals. Section II presents the basic FBG model. Section III presents the usual way to encode a FBG and the proposed spline encodings. Section IV presents the ES algorithm. Section V compares the performance of several encoding schemes through computer simulations. Finally, Section VI presents the conclusions.

II. FBG MODEL

Following the matrix formulation from [13], the refractive index profile is given in function of the axial distance z :

$$n(z) = n_{eff} + \nu \cos\left(\frac{4\pi n_{eff} z}{\lambda_B}\right), \quad (1)$$

where n_{eff} is the effective refractive index, ν the modulation parameter and λ_B is Bragg wavelength.

Using the coupled mode theory, it is possible to represent a uniform section of length Δz as a 2x2 matrix \mathbf{F} :

$$\begin{bmatrix} R_{\Delta z} \\ S_{\Delta z} \end{bmatrix} = \mathbf{F} \times \begin{bmatrix} R_0 \\ S_0 \end{bmatrix}, \quad (2)$$

where R_0 and S_0 represent respectively the field amplitudes of the propagating and back propagating modes at $z = 0$. $R_{\Delta z}$ and $S_{\Delta z}$ represent respectively the field amplitudes of the propagating and of the back propagating modes at $z = \Delta z$. \mathbf{F} is calculated in function of δ_n , ν , λ_B , Δz and n_{eff} .

A non uniform Bragg Grating, i.e., an apodized grating, can be modelled as a sequence of M uniform short gratings (uniform sections). Let \mathbf{F}_k be the transfer matrix of the k th section, where $k = 0$ for the first section at $z = 0$. The total transfer matrix for the apodized grating is given by multiplying all its M section matrices:

$$\mathbf{F}_T = \mathbf{F}_M \times \mathbf{F}_{M-1} \dots \times \mathbf{F}_{k+1} \times \mathbf{F}_k \times \mathbf{F}_{k-1} \dots \times \mathbf{F}_1 \times \mathbf{F}_0. \quad (3)$$

Now (2) can be rewritten in function of the total matrix \mathbf{F}_T :

$$\begin{bmatrix} R_L \\ S_L \end{bmatrix} = \mathbf{F}_T \times \begin{bmatrix} R_0 \\ S_0 \end{bmatrix}; \mathbf{F}_T = \begin{bmatrix} \mathbf{F}_{T11} & \mathbf{F}_{T12} \\ \mathbf{F}_{T21} & \mathbf{F}_{T22} \end{bmatrix}. \quad (4)$$

Where R_L and S_L represent respectively the field amplitudes of the propagating and of the back propagating modes at $z = L$. L is the total FBG length given by $L = \sum_{k=0}^{M-1} \delta z_k$.

The reflectance is given in function of \mathbf{F} elements by:

$$R = \left| \frac{-\mathbf{F}_{T21}}{\mathbf{F}_{T22}} \right|^2. \quad (5)$$

The apodized FBG can be represented in a vector form like $\mathbf{V} = \{\delta_{n0}, \nu_0, \lambda_{B0}, \Delta z_0, \dots, \delta_{nk}, \nu_k, \lambda_{Bk}, \Delta z_k, \dots, \delta_{nM-1}, \nu_{M-1}, \lambda_{BM-1}, \Delta z_{M-1}\}$, which is also a natural way to represent a FBG as an individual in meta-heuristics. In practical terms, not all parameters should be present in the vector because they could be constant or known for the entire grating. For example, the representation in the format $\{\nu_0, \nu_1, \dots, \nu_k, \dots, \nu_{M-1}\}$ was essentially the way chosen in [12] to represent individuals in the CMAES.

III. ENCODING STRATEGIES

Let us consider to be enough to represent ES individuals using $\mathbf{V} = \{\nu_0, \nu_1, \dots, \nu_k, \dots, \nu_{M-1}\}$. This encoding scheme will be referred here as direct encoding (DE), where the number of search space dimensions is equal to M , the same number of uniform sections. Satisfactory FBG representations make use of at least 20 sections for a centimetre long grating [10].

An interesting way to reduce the number of dimensions is through some sort of indirect encoding, where the individuals store few parameters in a vector form like $\mathbf{X} = \{x_0, x_1, \dots, x_j, \dots, x_{m-1}\}$ with $m < M$. Any ν_k can be calculated from \mathbf{X} using linear interpolation:

$$\nu_k = x_j + (x_{j+1} - x_j)(d_j - j), \quad (6)$$

where

$$d_j = m \times k / (M - 1) \quad (7)$$

and $j = \text{trunc}(d_j)$. Function $\text{trunc}()$ returns the integer part of an argument. The encoding scheme given by (6) will be referred as linear encoding or LE.

Another approach is to replace the linear interpolation by a spline approximation. This paper explores quadratic and cubic splines. For the quadratic spline encoding (QSE), ν_k can be calculated from \mathbf{X} as follows:

$$\nu_k = \begin{cases} \frac{(t-1)[(x_j+x_{j-1})(t-1)+4x_j t+(x_j+x_{j+1})t^2]}{2}, & 0 < j < m-1 \\ x_j + (x_{j+1} - x_j)[d_j - \text{trunc}(d_j)], & \text{otherwise} \end{cases} \quad (8)$$

where d_j is given by (7), $j = \text{round}(d_j)$ and $t = d_j - j + 0.5$. The function round returns the nearest integer of the argument.

For the cubic spline encoding (CSE), the relationship between ν_k and \mathbf{X} is given by:

$$\nu_k = \begin{cases} \frac{A(1-t)^3 + 6t(1-t)[B(1-t) + Ct] + Dt^3}{6}, & j < m-1 \\ x_j, & \text{otherwise} \end{cases} \quad (9)$$

where d_j is given by (7), $j = \text{trunc}(d_j)$ and $t = d_j - j$. Parameters A , B , C , and D are given respectively by:

$$A = \begin{cases} x_j, & j = 0 \\ x_{j-1} + 4x_j + x_{j+1}, & \text{otherwise} \end{cases}, \quad (10)$$

$$B = 2x_j + x_{j+1}, \quad (11)$$

$$C = 2x_{j+1} + x_j, \quad (12)$$

and

$$D = \begin{cases} x_j, & j \geq m-2 \\ x_j + 4x_{j+1} + x_{j+2}, & \text{otherwise} \end{cases}. \quad (13)$$

Indirect encoding strategies based on interpolations or approximations result in smoothed refractive index profiles as shown in Fig. 1, where the vector $\mathbf{X} = \{0.0, 0.25, 0.1, 0.7, 1.0, 0.7, 0.1, 0.25, 0.0\}$ was used to produce curves of $M = 200$. Smoothed profiles generates less undesired reflections which decreases the noise and minimizes undesired side lobes in the reflectance spectra. Furthermore, slow varying profiles are simpler to be manufactured than chaotic ones usually generated by direct encodings.

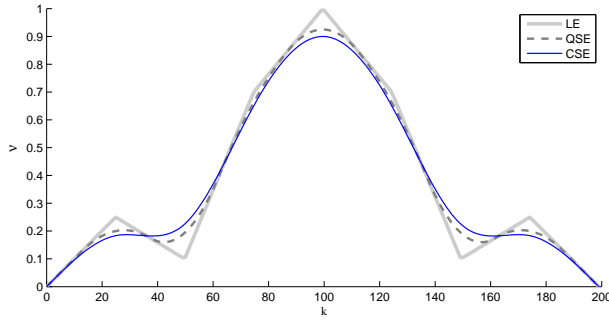


Fig. 1: ν profiles calculated using LE, QSE and CSE for $M = 200$, obtained from a test curve with $m = 9$.

IV. EVOLUTION STRATEGY

Evolution Strategies, among other meta-heuristics like GA, evolve individuals applying nature inspired operators. Back in 1970s, ES used to evolve a single individual by creating only one child each generation [14]. Modern versions of ES use a population of parents and differs from GA basically in the encoding and selection schemes [15].

The adapted modern version of ES used in this article could be defined as (S_A, S_B) -ES, where S_A and S_B are respectively the sizes of parent and child populations [16]. The algorithm is shown in Fig. 2. It starts creating two populations, **A** and **B**, to store respectively S_A and S_B individuals. Inside the generation loop (line 5), each individual of **B** is replaced by a new one made by the combination of intermediate crossover and Gaussian mutation. r in line 9 represents an uniform random value between 0 and 1. In this same line the function $P_C()$ returns the crossover probability based on A_1 rank, using Adaptive Genetic Algorithm (AGA) procedure defined in [17]. Hence the crossover operator is optionally applied in line 11 using A_1 and A_2 ($A_2 \neq A_1$) as parents. In line 12 the mutation is applied using as standard deviation the value returned by function $\delta()$. This function implements an adapted AGA procedure because the original one was not defined for Gaussian mutation:

$$\delta(A_1) = \begin{cases} \delta_1 \frac{\text{rank}(A_1)}{m}, & \text{rank}(A_1) < m \\ \delta_2 & \text{otherwise} \end{cases}, \quad (14)$$

where function $\text{rank}()$ returns the rank of an individual inside population **A** (it returns zero for the best and $S_A - 1$ for the worst), m is the rank of the individual whose fitness value is closest to the average, δ_1 and δ_2 are normalized deviation constants. In the line 14 all individual of population **A** are replaced by S_A individuals copied from **B**. The preparation for the next generation is complete after the elitist procedure from 15 to 18. Note in the line 18 that the individual A_b is inserted in **A**, which set the **A** size temporarily to $S_A + 1$ until **A** be reset in line 14 of the next generation.

The fitness calculation of each individual is based on the sum of squared errors between the target curve and the

-
01. Start **A** with S_A random individuals;
 02. Start **B** with S_B ($S_B > S_A$) individuals;
 03. Calculate the fitness for all individuals of **A**;
 04. Store the best **A** individual in A_b ;
 05. For each generation:
 06. For each **B** individual from **B**:
 07. Select a random individual A_1 from **A**;
 08. $B = A_1$;
 09. If $r < P_C(A_1)$:
 10. Select a random individual A_2 from **A**;
 11. $B = \text{Crossover}(A_1, A_2)$;
 12. $B = \text{Mutation}(B, \delta(A_1))$;
 13. Calculate the fitness of B ;
 14. Replace **A** by S_A best individuals from **B**;
 15. If A_b worse than **A** best:
 16. Update A_b ;
 17. If A_b better than **A** best:
 18. Insert A_b in **A**;
-

Fig. 2: ES algorithm.

reflectance spectrum. Let R_i be the i th reflectance value calculated for wavelength λ_i and T_i be the respective target value. The fitness value f can be calculated by

$$f = \sum_{i=1}^n (R_i - T_i)^2 \quad (15)$$

where n represents the number of samples used to build the reflectance curve. The ES of Fig. 2 minimizes f .

V. SIMULATIONS

In order to validate the proposed encoding schemes, the ES defined in the previous section IV was applied using direct encoding, LE, QSE and CSE. All following results were obtained using $S_A = 10$, $S_B = 40$, and $\delta_1 = \delta_2 = 0.01$. The maximum number of generations of 10000 was used as stop criteria.

Two projects were used to compare the proposed techniques. The first one was a FBG centred in $1.55\mu\text{m}$ and the second was TFBG from $1.5495\mu\text{m}$ to $1.5505\mu\text{m}$. The target curves of both are shown in Fig. 3. Note that the target curve for the FBG is not continuous. The interval from $1.5498\mu\text{m}$ to $1.5502\mu\text{m}$ is between two gaps of 0.05nm . They offer accommodation space for reflectance curves once abrupt targets are very difficult to fit.

The fitness in all simulations were calculated using (15) with $n = 100$. Samples are spaced uniformly in terms of wavelength inside the target region. If one sample drops inside a gap in the FBG target, it is not considered in the sum of (15). In all simulations the number of uniform sections used was 50 ($M = 50$).

For each project, for each encoding, the ES was tested 10 times with different random initial populations.

A. FBG project

For the FBG project, all sections used $\Delta z = 200\mu\text{m}$ and $\lambda_B = 1.55\mu\text{m}$. Indirect encoding schemes used $m = 5$ for ν .

Fig. 4 compares the ν profile and reflection curve for the best solutions synthesized by ES using LE, QSE and CSE for

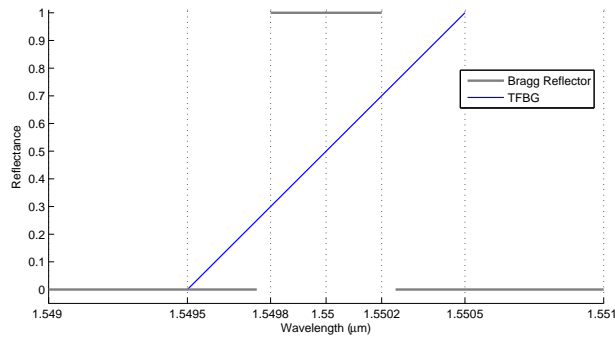


Fig. 3: Target curves for FBG and TFBG projects.

the Bragg reflector project. The linear interpolation bring the worst results among the indirect encoding schemes. QSE and CSE schemes give almost same results. Fig. 5 compares the results obtained for QSE with direct encoding (DE). Direct encoding achieved the best reflectance curve, but its ν profile is not as smooth as others obtained using QSE and CSE. It is interesting to observe how all profiles are near each other.

Fig. 6 shows the average evolution of fitness in function of generation number for ES using DE, QSE and CSE. Direct encoding has poor performance since spends more generations to reach convergence. This behavior was expected because ES using DE deals with 10 times more dimensions in search space than indirect encodings. The number of generations can be used safely as performance measurement parameter because the fitness function is called exactly 40 times each generation. Furthermore, the computational time spent in interpolations and spline approximations is negligible next the processing time spent in fitness calculations.

Table I shows performance parameters: best final fitness found in all 10 runs, worst fitness found, the mean and the standard deviation. It also shows the convergence number, i.e., the number of generations necessary to grant a fitness only 0.1% higher than the last generation best fitness.

TABLE I
FBG PERFORMANCE PARAMETERS

Parameter	DE	LE	QSE	CSE
Best	0.0286	0.05667	0.03690	0.03870
Mean	0.0314	0.05671	0.03692	0.03872
Worst	0.0424	0.05674	0.03695	0.03875
Deviation	1.76E-5	1.98E-5	1.60E-5	1.63E-5
Convergence	2812	208	185	141

B. TFBG project

For the TFBG project, all sections used $\Delta z = 400\mu\text{m}$ and linear chirp defined by the variation of λ_B in function of k . As stated in [12], the linear chirp is necessary in order to achieve the desired bandwidth of 1nm. But differently from [12], where the linear chirp was fixed, here it was defined

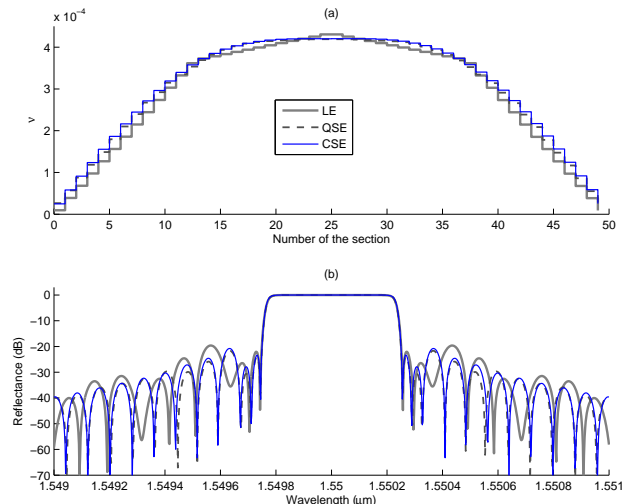


Fig. 4: ν profiles (a) and reflectance spectrum (b) for FBG synthesized using LE, QSE and CSE encodings.

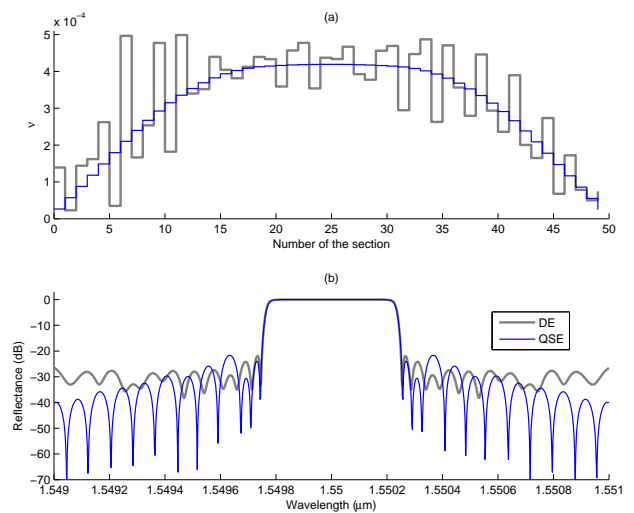


Fig. 5: ν profiles (a) and reflectance spectrum (b) for FBG synthesized using QSE and DE.

by ES itself by encoding λ_B in individuals using LE with $m = 2$. Thus, indirect encoded individuals were represented in vector form as $\{x_0, x_1, x_2, x_3, x_4, x_5, x_6, y_0, y_1\}$ with ν_k defined from x_0 to x_6 by (6), (8) or (9) using $m = 7$ and with λ_k given from y_0 and y_1 by (6) (replacing x_k by y_k). For direct encoding, the individuals were represented in vector form as $\{\nu_0, \nu_1, \dots, \nu_k, \dots, \nu_{M-2}, \nu_{M-1}, y_0, y_1\}$, with λ_k given from y_0 and y_1 by (6) in the same way as in indirect encoding.

Fig. 7 compares the ν profile and reflection curve for the best solutions synthesized by ES using LE and QSE and CSE for the TFBG project. As observed in the Bragg

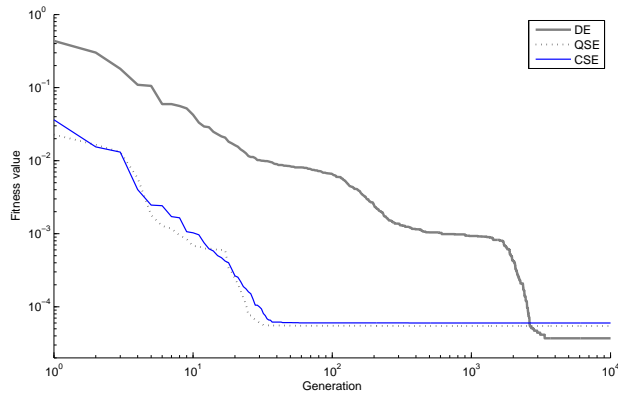


Fig. 6: Average curves of fitness value in function of generation number for QSE, CSE and DE.

reflector project, the linear interpolation brings the worst results among all studied indirect encoding schemes. QSE and CSE are similar each other. Fig. 8 compares the results obtained for QSE with direct encoding. Differently from the Bragg reflector project, the direct encoding resulted worse than indirect ones. In the other hand, the chirp obtained for DE was only 0.1062nm/mm , lower in magnitude when compared to -0.7893nm/mm for LE, 0.7817nm/mm for QSE and 0.7743nm/mm for CSE. The minus signal for LE chirp indicates a decreasing λ_B toward the last section of FBG and explain the inverted ν profile. Since no restrictions were imposed concerning the chirp signal, negative and positive values were obtained evenly for all encodings.

Fig. 9 shows the average evolution of the best fitness in function of generation number for ES using direct encoding, QSE and CSE. Differently from the FBG project, the direct encoding typically ends its evolution early, probably trapped near some local optimum after 1000 generations. QSE and CSE show close performances with QSE being slightly better.

Table II shows performance parameters for TFBG project. As observed in the FBG project, the QSE is again the best among all indirect encoding schemes, although its fitness standard deviation resulted slightly inferior when comparing to CSE. In Table II for indirect encodings the convergence occurs with more generations than observed in Table I. It is not a surprising result because the number of dimensions in TFBG project was 9 against 5 in FBG project. For direct encoding, the reduction of the convergence parameter observed can be explained only by premature convergence. TFBG project is really a more complex project to synthesize (with an increase of 2 dimensions in search space) than FBG and it would demand an ES with larger population in order to achieve better results using DE.

VI. CONCLUSIONS

Spline encodings combined to a modified evolutionary strategy have been successfully applied in the FBG synthesis.

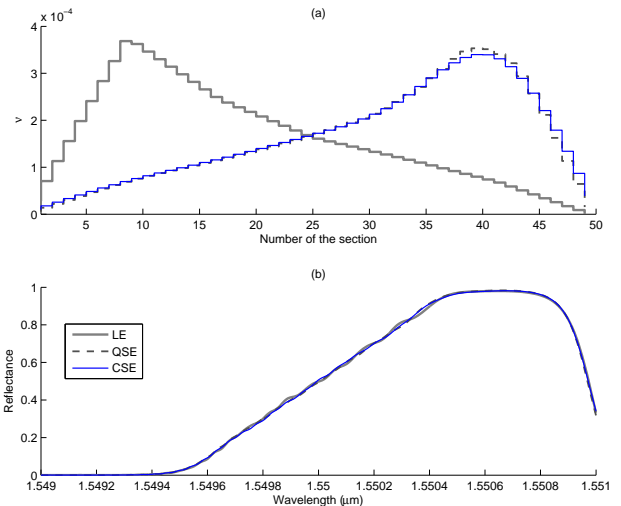


Fig. 7: ν profiles (a) and reflectance spectrum (b) for TFBG synthesized using LE, QSE and CSE encodings.

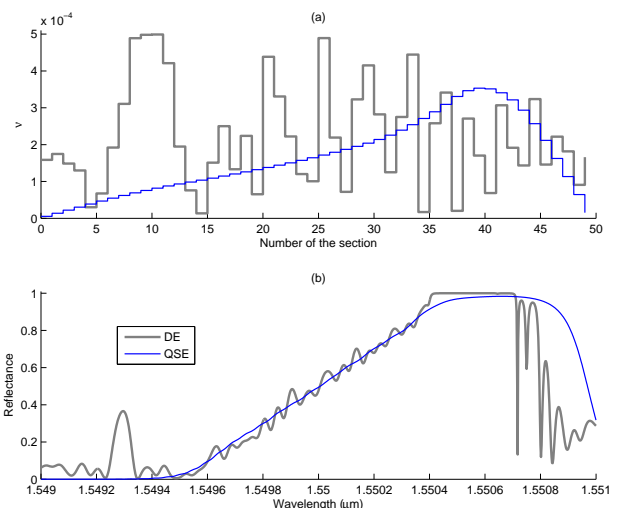


Fig. 8: ν profiles (a) and reflectance spectrum (b) for TFBG synthesized using QSE and DE.

Two projects have been considered and comparisons involving quadratic and cubic spline encodings, direct encoding, and linear encoding have been provided. It has been shown that spline schemes are able to reduce the number of dimensions and generate attractive softened refractive index profiles.

Quadratic spline encoding (QSE) should always be considered in detriment of cubic encoding (CSE) because it is simpler, has comparable performance and give better results.

However, spline encodings are not free of issues. If the search space is too much simplified, the possible solutions can loose its flexibility. That occurred in the simple FBG

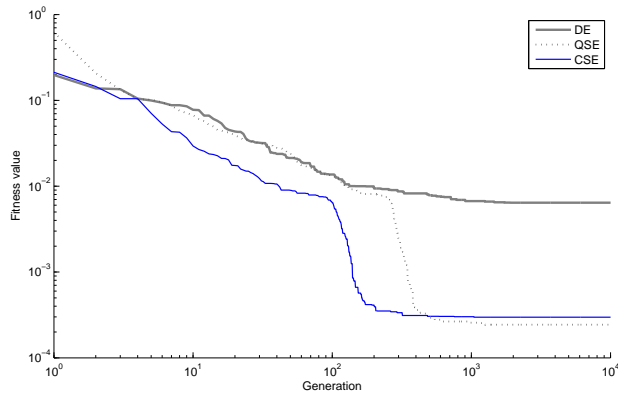


Fig. 9: Average curves of fitness value in function of generation number for QSE, CSE and DE.

TABLE II
TFBG PERFORMANCE PARAMETERS

Parameter	DE	LE	QSE	CSE
Best	0.3307	0.0878	0.0739	0.0776
Mean	0.3836	0.5836	0.0798	0.0840
Worst	0.4537	0.8120	0.0889	0.0891
Deviation	0.0408	0.3430	0.0043	0.0033
Convergence	1065	396	902	761

project where the direct encoding overcame indirect encoding schemes. Nevertheless the results from spline schemes are more attractive due its simpler profiles. An interesting possibility to conciliate performance and flexibility would be to use spline encoding to achieve an initial solution for further application of a direct encoded meta-heuristic or another suitable optimization technique.

The definition of m parameter in indirect encodings was accomplished based on a trial and error procedure. A better way to do that could be through a progressive spline encoding scheme where the number of parameters m would be increased gradually whenever the population diversity drops below a threshold. This technique would require the insertion of new random parameters in individuals in the middle of optimization process, probably in a very similar way as performed in [18].

REFERENCES

- [1] K. A. Winick and J. E. Roman. Design of corrugated waveguide filters by fourier transform techniques. *IEEE Journal of Quantum Electronics*, 26:1918–1929, 1990.
- [2] Johannes Skaar and Ole Henrik Waagaard. Design and characterization of finite-length fiber gratings. *IEEE Journal of Quantum Electronics*, 39:1238–1245, 2003.
- [3] Ming Li, Junya Hayashi, and Hongpu Li. Advanced design of a complex fiber bragg grating for a multichannel asymmetrical triangular filter, 2009.
- [4] B. Malo, K. O. Hill, F. Bilodeau, D. C. Johnson, and J. Albert. Point-by-point fabrication of micro-bragg gratings in photosensitive fiber using single excimer pulse refractive-index modification techniques. *Electronic Letters*, 29:1668–1669, 1993.

- [5] K. Aksnes and J. Skaar. Design of short fiber bragg gratings by optimization. *Applied Optics*, 43:2226–2230, 2004.
- [6] David E. Goldberg. *Genetic Algorithms in Search, Optimization, and Machine Learning*. Addison-Wesley Professional, January 1989.
- [7] J. Kennedy and R. C. Eberhart. Particle swarm optimization. In *Proceedings of IEEE Conference of Neural Networks IV*, 1995.
- [8] Johannes Skaar and Knut Magne Risvik. A genetic algorithm for the inverse problem in synthesis of fiber gratings. *IEEE Journal of Lightwave Technology*, 16:1928–1932, 1998.
- [9] S. Baskar, A. Alphones, P. N. Suganthan, N. Q. Ngo, and R. T. Zheng. Design of optimal length low-dispersion FBG filter using covariance matrix adapted evolution. *IEEE Photonics Technology Letters*, 17:2119–2121, 2005.
- [10] S. Baskar, R. T. Zheng, A. Alphones, N. Q. Ngo, and P. N. Suganthan. Particle swarm optimization for the design of low-dispersion fiber bragg gratings. *IEEE Photonics Technology Letters*, 17:615–617, 2005.
- [11] Rui Huang, Yingwu Zhou, Haiwen Cai, Ronghui Qu, and Zujie Fang. A fiber bragg grating with triangular spectrum as wavelength readout in sensor systems. *Optics Communications*, (229):197–201, 2004.
- [12] S. Baskar, P. N. Suganthan, N. Q. Ngo, A. Alphones, and R. T. Zheng. Design of triangular FBG filter for sensor applications using covariance matrix adapted evolution algorithm. *Optics Communications*, (260):716–722, 2006.
- [13] Turan Erdogan. Fiber grating spectra. *Journal of Lightwave Technology*, 15:1277–1294, 1997.
- [14] Thomas Bck and Schwefel. Evolutionary computation: an overview. In *International Conference on Evolutionary Computation*, 1996.
- [15] Z. Michalewicz. *Genetic Algorithms + Data Structures = Evolution Programs*. Springer-Verlag, 1992.
- [16] Thomas B. and H-P. Schwefel. Evolutionary computation: comments on the history and current state. *IEEE Transactions on Evolutionary Computation*, 1:3–17, 1997.
- [17] Zhiming Liu, Jiliu Zhou, and Su Lai. New adaptive genetic algorithm based on ranking. In *Proceedings of the Second International Conference on Machine Learning and Cybernetics*, pages 1841–1844, 2003.
- [18] Il Yong Kim and Olivier de Weck. Progressive structural topology optimization by variable chromosome length genetic algorithm. In *The Third China-Japan-Korea Joint Symposium on Optimization of Structural and Mechanical Systems*, 2004.